An auto-biotinylated bifunctional protein nanowire for ultra-sensitive molecular biosensing ☆

Dong Men [a,d], Zhi-Ping Zhang [a], Yong-Chao Guo [b], Duan-Hao Zhu [a,d], Li-Jun Bi [c], Jiao-Yu Deng [a], Zong-Qiang Cui [a], Hong-Ping Wei [a], Xian-En Zhang [a,*]

[a] State Key Laboratory of Virology, Wuhan Institute of Virology, Chinese Academy of Sciences, Wuhan 430071, PR China
[b] Department of Chemical and Biomolecular Engineering, The Hong Kong University of Science and Technology, Clear Water Bay, Kowloon, Hong Kong
[c] National Laboratory of Biomacromolecules, Institute of Biophysics, Chinese Academy of Sciences, Beijing 100101, PR China
[d] Graduate School, Chinese Academy of Sciences, Beijing 100039, PR China

ARTICLE INFO

ABSTRACT

In order to obtain an ultra-sensitive molecular biosensor, we designed an auto-biotinylated bifunctional protein nanowire (bFPNw) based on the self-assembly of a yeast amyloid protein, Sup35, to which protein G and a biotin acceptor peptide (BAP) were genetically fused. These auto-biotinylated bFPNws can transfer hundreds of commercially available diagnostic enzymes to an antigen–antibody complex via the biotin–avidin system, greatly enhancing the sensitivity of immune-biosensing. Compared to our previously reported seeding-induced bFPNws (Men et al., 2009), these auto-biotinylated bFPNws gave greater signal amplification, reduced non-specific binding and improved stability. The auto-biotinylated self-assembled bFPNw molecular biosensors were applied to detect *Yersinia pestis* (*Y. pestis*) F1 antigen and showed a 2000- to 4000-fold increase in sensitivity compared to traditional immunoassays, demonstrating the potential use of these self-assembling protein nanowires in biosensing.

© 2010 Elsevier B.V. All rights reserved.

1. Introduction

There is substantial interest in the use of biosensing to detect pathogens or biomarkers for cancers and other diseases at ultralow levels. Recently, nanomaterials such as quantum dots (Chan et al., 2002), gold nanoparticles (Nam et al., 2003), carbon nanotubes (Chen et al., 2008) and silicon nanowires (Zheng et al., 2005) have been widely used in biosensing and have substantially improved sensitivity. However, most of these materials require complex and expensive chemical modification before they can be applied in biosensors. For example, nanomaterials must be conjugated with antibodies and nucleic acids to capture target molecules. Compared with inorganic materials, biomaterials such as DNA (Feldkamp and Niemeyer, 2006) and proteins (Zhang, 2009) offer great potential for use as scaffolds in the building of functional nanostructures while avoiding the need for chemical modifications.

Self-assembling proteins are attractive alternative natural nanomaterials for several reasons. Firstly, proteins are natural nanomachines and nanoscale-architectural components that can be formed into numerous functional nanoscale-structures by natural self-assembly processes (Zhang, 2003). Molecular self-assembly (MSA) can be used to carry out many of the most difficult steps in nanofabrication (Whitesides and Grzybowski, 2002). Secondly, proteins are very diverse and fulfill a broad range of functions via highly specific interactions. In addition, proteins are easy to manipulate via genetic methods. Together, these properties contribute to the great potential offered by protein-based nanostructures in nanotechnology.

Amyloid proteins are self-assembling proteins which form well-ordered fibrillar aggregates that are called amyloid fibrils (Chiti and Dobson, 2006). Amyloid fibrils are widely observed in association with various acquired and hereditary disorders including Alzheimer's disease, type 2 diabetes and prion diseases (Chien et al., 2004). In a previous study, we constructed a bFPNw molecular biosensor based on the seeding events that occur in amyloid fibre growth *in vitro*. Protein G and methyl parathion hydrolase (MPH) were fused to the prion domain of the amyloid protein, Sup35, of *Saccharomyces cerevisia*. The resultant bFPNw possessed a high ratio of enzyme to protein G, allowing a dramatic increase in the enzymatic signal when protein G bound to an antibody target. Compared to conventional enzyme-linked immunosorbent assays (ELISAs) using enzyme-conjugated secondary antibodies, this bFPNw molecular biosensor enhanced sensitivity 100 times (Men et al., 2009).

Although this design shows great potential for use in biosensing, it has several drawbacks that affect its practical application. Firstly, MPH is not commercially available, greatly limiting its application. The activity of MPH is also lower than that of commercially available diagnostic enzymes such as HRP or AP, resulting in a longer colour development reaction time and a lower signal intensity. Secondly, there are no separation steps in the preparation method to remove improperly assembled components, which is the main reason for the observed signal instability. Finally, sonication, which is used in the preparation of amyloid seeds, reduces the antibody-binding activity of protein G. Here, to circumvent these problems, we constructed novel auto-biotinylated bFPNws which had greatly improved biosensing. Commercially available diagnostic enzymes and a substrate system were employed alongside the biotin–avidin system which was introduced using a BAP tag and biotin holoenzyme synthetase (BirA). BirA is a bifunctional enzyme that adenylates biotin and then uses the reactive biotinyl-50-AMP product to transfer biotin to the biotin carboxyl carrier protein (BCCP) in *Escherichia coli* (*E. coli*) (Wilson et al., 1992). The BAP tag is the substrate of BirA (Howarth and Ting, 2008). Our new bFPNw construction method avoids reduction of the binding ability of protein G, amplifies the signal, decreases background noise and enhances signal stability.

2. Materials and methods

2.1. Chemicals and reagents

Streptavidin-peroxidase polymer (SA-HRP) and a 3,3′,5,5′-tramethyl-benzidine (TMB) liquid substrate system for ELISA were obtained from Sigma–Aldrich (St Louis, MO, USA). HRP-labeled secondary antibodies were obtained from Santa Cruz (Santa Cruz, CA, USA). Other chemicals and reagents were purchased from Sinopharm Chemical Reagent Corp. (Shanghai, China), unless otherwise noted. Additional details can be found in supplementary information.

2.2. Preparation of the fusion protein

The BirA (EC 6.3.4.15) gene was amplified from the genome of *E. coli* BL21 by PCR and cloned into the pCDFDuet vector (compatible with pET28) to give pCDFDuet-BirA. The plasmids, pET28-Sup35-BAP and pET28-Sup35-SPG, were constructed using the previously described pET28-Sup35[1–61] (Men et al., 2009). The prion domain of Sup35 (Sup35[1–61]), green fluorescent protein (GFP) and a spacer peptide were cloned in order into pET28 to give pET28-Sup35. The IgG binding domain, C1, of protein G from *Streptococcus*, here referred to as SPG, was amplified by PCR (Gronenborn et al., 1991). The BAP tag (Beckett et al., 1999) and SPG were inserted into the 5′-terminal end of the pET28-Sup35 plasmid to construct pET28-Sup35-BAP and pET28-Sup35-SPG, respectively. The plasmid map of pET28-Sup35-BAP is shown in Fig. 1A.

The fusion protein Sup35-SPG was expressed in *E. coli* BL21 and purified as previously described (Men et al., 2009). The constructed pCDFDuet-BirA and pET28-Sup35-BAP plasmids were co-transformed into *E. coli* BL21. Transformed *E. coli* cells were added to LB medium in the presence of 50 μg/ml streptomycin, 50 μg/ml kanamycin and 12 μg/ml biotin (Sigma–Aldrich). The remaining steps of Sup35-BAP expression and purification were the same as those for Sup35-SPG (Men et al., 2009). The expression and biotinylation of Sup35-SPG were measured by SDS-PAGE and Western blotting, respectively (supplementary information).

2.3. Construction of auto-biotinylated bFPNws

Our Sup35-BAP nanowires were formed by Sup35-BAP seed induction. Sup35-BAP seeds were produced by sonicating Sup35-
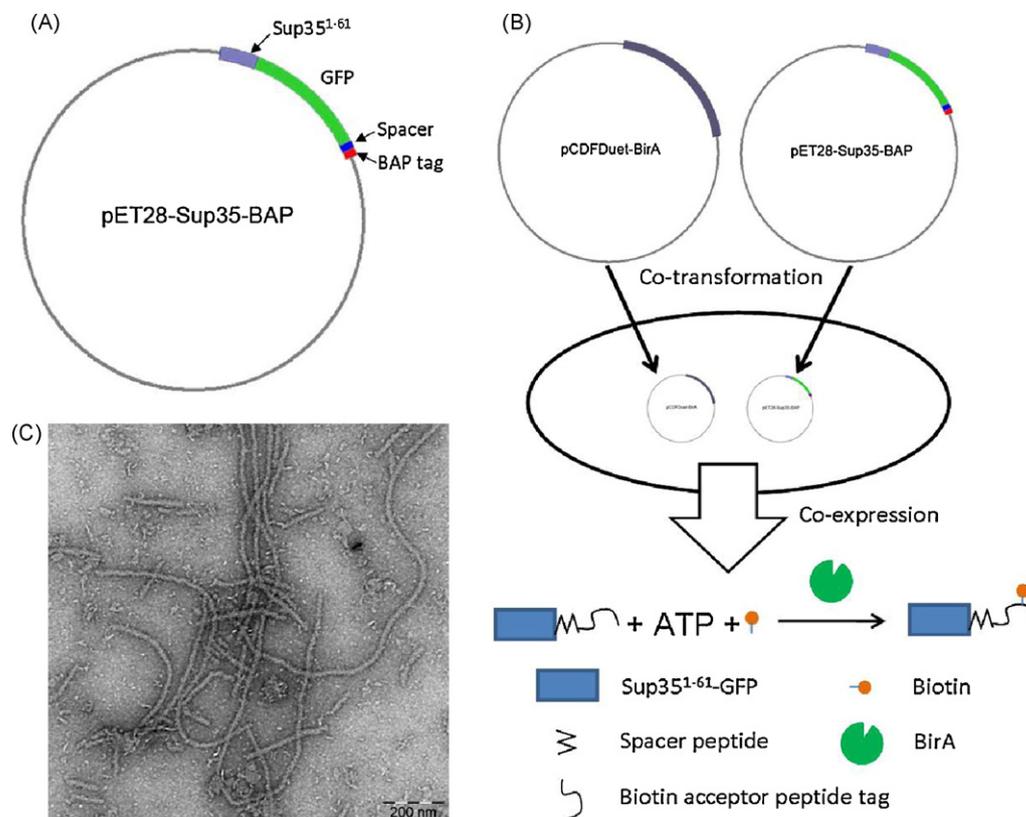
Fig. 1. The auto-biotinylated self-assembled fusion protein Sup35-BAP. (A) pET28-Sup35-BAP plasmid map. (B) Auto-biotinylation of Sup35-BAP *in vivo*. (C) Electron micrograph of auto-biotinylated self-assembled nanowires. Bar = 200 nm.

BAP aggregates, which were preformed by incubating purified Sup35-BAP at 4 °C for 5 days. The formation of the Sup35-BAP nanowires was controlled by maintaining the ratio of the Sup35-BAP seeds to Sup35-BAP monomers at 1:4 (w/w). Sup35-BAP nanowires were separated by centrifugation and then added to a Sup35-SPG monomer solution at room temperature for 10 min. The resulting nanowires were harvested by centrifugation and diluted 10 times with 0.5% PBS-milk. Further details are given in supplementary information.

2.4. Auto-biotinylated bFPNw immunoassay

The auto-biotinylated bFPNw immunoassay was based on the principle of indirect ELISA. The antigen was coated on a microplate and blocked with 5% milk. After incubating the antigen-coated microplate with a primary antibody, 100 μl bFPNws was added to each well. The microplate was incubated at 37 °C for 1 h to allow the bFPNws to bind to the antigen–antibody complexes, and then each well was washed to remove the unbound nanowires. A 2 μg/ml SA-HRP working solution prepared by dilution with phosphate buffered saline (PBS) buffer solution containing 0.5% milk. This SA-HRP solution was added in volumes of 100 μl to each well of the microplate. The microplate was incubated at room temperature for 50 min and washed repeatedly (see supplementary information). Detection results were analyzed using a TMB liquid substrate system and the optical absorption was measured at a wavelength of 450 nm in a microplate reader (Synergy HT, BIO-TEK).

3. Results and discussion

3.1. Characterization of the auto-biotinylated fusion proteins

Sup35-BAP was chosen as the backbone of the bFPNw to link the nanowire with commercial avidin-enzyme conjugates. Its self-assembly into nanowires was driven by the prion domain of Sup35. The BAP tag was biontinylated by BirA during Sup35-BAP expression (Fig. 1B) and resulted in the surface of the Sup35-BAP nanowire being fully biotinylated. To ensure that the BAP tag was located on the surface of the nanowire, a spacer peptide was inserted into the N-terminal region of the BAP tag. The BirA gene was co-transformed with Sup35-BAP to ensure the *in vivo* biotinylation of the BAP fusion protein (Smith et al., 1998). The expression of Sup35-BAP was measured by SDS-PAGE. The BirA and Sup35-BAP protein were co-expressed by induction with isopropyl β-D-1-thiogalactopyranoside (IPTG) (Fig. 2A, lane 2). The extent of biotinylation was evaluated using SA-HRP and a biotinylated anti-GFP antibody. The extent of biotin modification of BAP and GFP could be compared by Western blotting (Fig. 2A, lanes 4 and 5), since the ratio of GFP and BAP in Sup35-BAP was 1:1. Results indicated that Sup35-BAP was biotinylated efficiently. In the final step, the purified Sup35-BAP was incubated at 4 °C for 1 week to allow self-assembly to occur. A large number of filaments were observed in the Sup35-BAP solution by transmission electron microscopy (TEM) (Fig. 1C). The average diameter of these filaments was approximately 17.5 ± 1 nm, with a length of up to several micrometers, indicating that fusion of the lig-
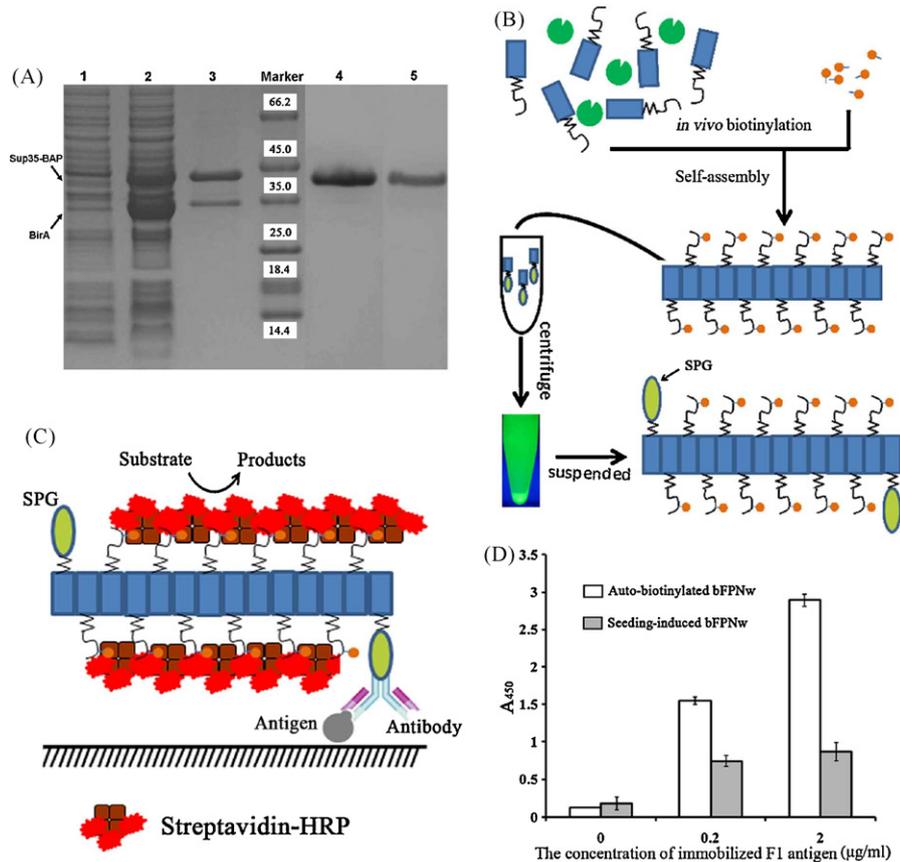
Fig. 2. Construction of auto-biotinylated bFPNws. (A) SDS-PAGE and Western blotting analysis of Sup35-BAP. Lane 1, total cellular proteins after incubation of Sup35-BAP and BirA for 2 h; lane 2, total cellular proteins after induction by IPTG for 10 h; lane 3, purified Sup35-BAP; lane 4, purified Sup35-BAP stained with SA-HRP; lane 5, purified Sup35-BAP detected with a biotinylated anti-GFP antibody and SA-HRP. (B) Construction of auto-biotinylated bFPNws. (C) Auto-biotinylated bFPNw-mediated immunoassays. (D) Functional evaluation and comparison of auto-biotinylated bFPNws and seeding-induced bFPNws. Indirect ELISA was performed to evaluate the antibody-capturing and streptavidin-binding ability of auto-biotinylated bFPNws using the F1 antigen.

and to Sup35p did not impair the formation of the nanowires. The length of the Sup35-BAP nanowires could be controlled by adjusting the ratio of preformed Sup35-BAP seeds to Sup35-BAP monomers. The length of Sup35-BAP nanowires used in this study was about 400 nm at a ratio of seeds to monomers of 1:4 (supplementary information Fig. 1).

3.2. Construction of bifunctional nanowires

Fig. 2B illustrates the construction of auto-biotinylated bFPNws. In our previous study, the ratio of capture molecules (protein G) to signal molecules (MPH) was controlled by adjusting the weight ratio of protein G seeds to MPH monomers. The activity of protein G was affected by sonication during seed preparation and decreased its antibody-binding ability. To avoid this problem, the prepared Sup35-BAP nanowires were used as "seeds" to induce Sup35-SPG growth on the end of the Sup35-BAP nanowires. Although the current method also requires sonication in the Sup35-BAP seed preparation step, the biotin ligand was not affected much because biotin is a small molecule and is covalently attached to the lysine residue of the BAP.

The prepared biotinylated nanowires were separated by centrifugation. The unassembled monomers were removed by discarding the supernatant and repeating the wash steps. When centrifuge speed was optimized, we found that the pellet could endure the washing step and the re-suspension of the pellet, with centrifugation at $10,000 \times g$ for 10 min (supplementary information).

The resuspended Sup35-BAP nanowires were added to the Sup35-SPG monomer solution to induce Sup35-SPG assembly onto the ends of the biotinylated nanowires. Since SPG is one of the three IgG binding domains of protein G, a suitable number of SPG molecules should be attached to the ends of the bFPNw since the number of SPG molecules is related to the binding ability of the nanowire to antigen–antibody complexes; the signal molecule: capture molecule ratio will be reduced if there are too many SPG molecules, thus affecting signal amplification. The number of attached SPG molecules can be controlled by varying the growth time. SPG growth was monitored by streptavidin-modified magnetic beads and HRP-labeled antibody (supplementary information Fig. 3A). Results showed that the amount of SPG attached to the end of the Sup35-BAP nanowires increased for the first 10 min, after which growth proceeded slowly (supplementary information Fig. 3B). For this reason, bFPNws were collected by centrifugation after 10 min of SPG growth.

3.3. Auto-biotinylated bFPNw immunoassay

To evaluate the biological function of the auto-biotinylated bFPNws, the prepared bFPNws were subjected to a typical ELISA procedure (Fig. 2C). The availability of many biotin molecules which can bind to SA-HRP molecules on the surface of the auto-biotinylated bFPNws, and the binding of SPG molecules at the ends of the bFPNws to the Fc fragments of detection antibodies, results in a large number of SA-HRP molecules per antigen–antibody complex. As a control, the seeding-induced bFPNws immunoassay was performed at the same time, using our previously described protocol (Men et al., 2009). As expected, the signal intensity of the auto-biotinylated bFPNws was directly correlated to the concentration of the F1 antigen that was immobilized on the wells (Fig. 2D). Compared with seeding-induced bFPNws, the auto-biotinylated bFPNws showed a stronger signal intensity, lower background noise and better signal stability (Fig. 2D). There are three reasons for this result. Firstly, the higher activity of the commercial diagnostic enzyme greatly enhanced the signal intensity and decreased the time of the colour development reaction (less than 1 min),

inhibiting the generation of background noise. Secondly, the signal was more stable since most unassembled or incorrectly assembled components were removed by the separation steps during bFPNw preparation. Thirdly, SPG was not affected by sonication, and thus the bFPNws could endure higher washing intensities, which is helpful in decreasing the background signal.

To further demonstrate the power of the auto-biotinylated bFPNw-based detection system over conventional immunoassays, parallel assays (one using a HRP-labeled secondary antibody, and one using a biotin-labeled secondary antibody) were performed on a pathogen F1-modified microplate. As shown in Fig. 3, the detection limit of the auto-biotinylated bFPNw was found to be 0.1 ng/ml (6 pmol/l), at an OD cut-off value of 0.2 and a signal to noise ratio (S/N) of ≥2. This indicates that the sensitivity of F1 detection using auto-biotinylated bFPNws was 2000- to 4000-fold higher than that of conventional ELISA, and the detection limit was improved from the 200 ng/ml in both conventional ELISA methods to 0.1–0.05 ng/ml for auto-biotinylated bFPNws. This extraordinarily high sensitivity may be due to the large number of enzyme molecules carried by the bFPNws, significantly greater than the number of either HRP or biotin-labeled secondary antibody molecules in conventional ELISA methods.

The biotinylation of nanowires mimics a biological process which occurs spontaneously during protein expression. Compared with chemical methods used in the modification of nanomaterials, biological modification is site-specific, homogeneous and low-cost. In addition to biotinylation, site-specific atomic-level modifications, such as phosphorylation, methylation and acetylation, are widespread in living organisms. Mimicking these *in vivo* processes is a useful approach in nanofabrication (Sarikaya et al., 2003). *In vivo* modification of proteins and protein self-assembly are new approaches for controlling the orientation of enzyme–antibody coupling. In biosensing, most multi-functional biomolecular complexes are cross-linked or immobilized by chemical conjugation. In most circumstances, however, this conjugation requires the use of a large amount of enzyme. Conjugated bio-
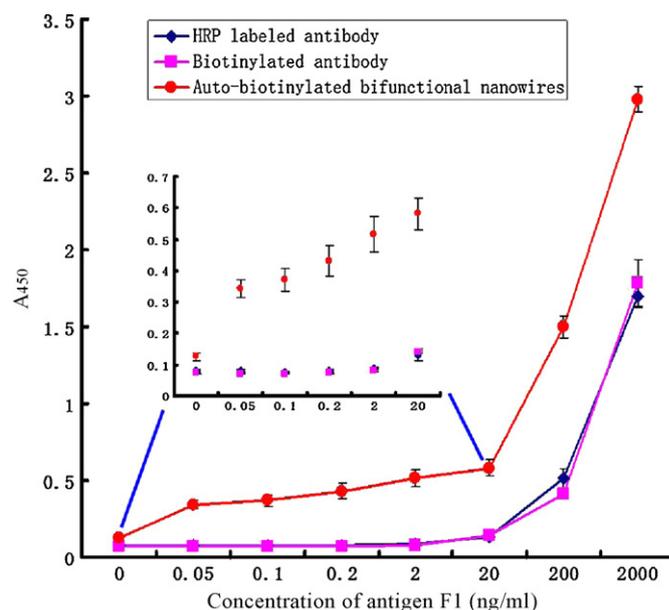
Fig. 3. Comparison of the sensitivity of our auto-biotinylated bFPNw molecular biosensor with that of conventional indirect ELISAs using HRP-labeled antibodies and biotinylated antibodies for F1 antigen detection. The detection procedure was similar to that for indirect ELISAs. Colour development achieved by HRP was measured at a wavelength of 450 nm on a microplate reader (BIO-TEK). The detection limit of the auto-biotinylated bFPNws was found to be 0.1 ng/ml (6 pmol/l) at an OD cut-off value of 0.2 and an S/N of ≥2.

molecules very often also show reduced activity. This is mainly due to the multi-site attachment, multiple orientations, and steric hindrance that result from random chemical crosslinking (Shao et al., 2000). *In vivo* bio-processing and self-assembly methods successfully control biomolecular orientation by genetic engineering, keeping the conjugated bio-molecules ordered, homogeneous and working effectively (Shi et al., 2004).

Although auto-biotinylated bFPNws show great potential for biosensing, some problems with the technology still remain. The most important issue is that it is difficult to use bFPNws in sandwich ELISA processes since protein G binds to the Fc fragment of antibodies from many species. It is expected that this problem can be resolved by changing the capture molecule; suitable capture molecules are currently being designed in our laboratory. The shorter nanowires used in this study gave a stable signal, but greater nanowire homogeneity is still required to realize quantitative detection. We expect that this can be achieved by improving the preparation method and incorporating more stringent quality control. Non-specific adsorption caused by the large surface area of the protein nanowires still remains a problem. We are currently examining two possible solutions; selecting the molecules exposed on the surface of the nanowire to reduce non-specific binding, and developing special washing methods (for example, the fluidic force discrimination method) which can reduce the non-specific binding of nanowires by discriminating different binding abilities.

4. Conclusion

A novel self-assembling bFPNw was developed by mimicking *in vivo* biotinylation. By using commercially available diagnostic enzyme and substrate systems, the auto-biotinylated bFPNws were used in *Y. pestis* F1 antigen detection, and showed a 2000- to 4000-fold increase in sensitivity over traditional immunoassays. The self-assembly of amyloid proteins offers a new route for the production of protein-based functional nanowires.

Appendix A. Supplementary data

Supplementary data associated with this article can be found, in the online version, at doi:10.1016/j.bios.2010.07.103.

References

Beckett, D., Kovaleva, E., Schatz, P.J., 1999. Protein Sci. 8 (4), 921–929.
Chan, W.C., Maxwell, D.J., Gao, X., Bailey, R.E., Han, M., Nie, S., 2002. Curr. Opin. Biotech. 13 (1), 40–46.
Chen, Z., Tabakman, S.M., Goodwin, A.P., Kattah, M.G., Daranciang, D., Wang, X., Zhang, G., Li, X., Liu, Z., Utz, P.J., Jiang, K., Fan, S., Dai, H., 2008. Nat. Biotechnol. 26 (11), 1285–1292.
Chien, P., Weissman, J.S., DePace, A.H., 2004. Annu. Rev. Biochem. 73, 617–656.
Chiti, F., Dobson, C.M., 2006. Annu. Rev. Biochem. 75, 333–366.
Feldkamp, U., Niemeyer, C.M., 2006. Angew. Chem. Int. Edit. 45 (12), 1856–1876.
Gronenborn, A.M., Filpula, D.R., Essig, N.Z., Achari, A., Whitlow, M., Wingfield, P.T., Clore, G.M., 1991. Science 253 (5020), 657–661.
Howarth, M., Ting, A.Y., 2008. Nat. Protoc. 3 (3), 534–545.
Men, D., Guo, Y.C., Zhang, Z.P., Wei, H.P., Zhou, Y.F., Cui, Z.Q., Liang, X.S., Li, K., Leng, Y., You, X.Y., Zhang, X.E., 2009. Nano Lett. 9 (6), 2246–2250.
Nam, J.M., Thaxton, C.S., Mirkin, C.A., 2003. Science 301 (5641), 1884–1886.
Sarikaya, M., Tamerler, C., Jen, A.K., Schulten, K., Baneyx, F., 2003. Nat. Mater. 2 (9), 577–585.
Shao, W.H., Zhang, X.E., Liu, H., Zhang, Z.P., 2000. Bioconjugate Chem. 11 (6), 822–826.
Shi, J.X., Zhang, X.E., Xie, W.H., Zhou, Y.F., Zhang, Z.P., Deng, J.Y., Cass, A.E., Zhang, Z.L., Pang, D.W., Zhang, C.G., 2004. Anal. Chem. 76 (3), 632–638.
Smith, P.A., Tripp, B.C., DiBlasio-Smith, E.A., Lu, Z.J., LaVallie, E.R., McCoy, J.M., 1998. Nucleic Acids Res. 26 (6), 1414–1420.
Whitesides, G.M., Grzybowski, B., 2002. Science 295 (5564), 2418–2421.
Wilson, K.P., Shewchuk, L.M., Brennan, R.G., Otsuka, A.J., Matthews, B.W., 1992. Proc. Natl. Acad. Sci. U.S.A. 89 (19), 9257–9261.
Zhang, S.G., 2003. Nat. Biotechnol. 21 (10), 1171–1178.
Zhang, X.E., 2009. J. Biosci. Bioeng. 108, S2–S12.
Zheng, G.F., Patolsky, F., Cui, Y., Wang, W.U., Lieber, C.M., 2005. Nat. Biotechnol. 23 (10), 1294–1301.